

Some Behaviors and Characteristics of Decarburized Layer in Spheroidal Graphite Cast Iron

Susumu YAMADA*, Toshiyuki KONNO*, Shoji GOTO**,
Setsuo ASO** and Yoshinari KOMATSU**

*Chuo Malleable Iron Co., Ltd,
4 Hirako, Asada-cho, Nisshin-city 470-0124 Aichi-prefecture Japan
E-mail : yamada@chuokatan.co.jp

**Faculty of Engineering and Resource Science, Akita University,
1-1 Tegata Gakuen-cho Akita city 010-8502 Akita prefecture Japan

Spheroidal graphite cast irons are widely used for auto parts because they have large degrees of freedom in shape and are inexpensive. When they are welded, however, they show serious drawback of crack generation due to excess carbon at the hardened region of heat-affected zone. We have studied on decarburized spheroidal graphite cast iron which has a possibility of welding because of graphite free in the surface region. In the present study, some characteristics of the decarburized layer in the spheroidal graphite cast iron were investigated. The results obtained are as follows.

Growth of decarburized layer is controlled by diffusion of carbon atoms toward the surface region in the iron during the heat-treatment and there is a critical temperature of 930 K for the decarburization, below which decarburization does not occur. When the area ratios of the decarburized layer to whole sectional area in the rod-shaped tensile test specimen was defined to be a ratio of decarburized layer, the tensile strength of the specimen scarcely influenced by the ratio of decarburized layer. However, when the overdecarburization was processed, the tensile strength showed a tendency to decrease.

Therefore, it should be noted in practical use of the decarburized spheroidal graphite cast iron that the excessive decarburization makes the strength of thin parts of the iron to decrease.

Key Words : spheroidal graphite cast iron, welding, decarburization, diffusion, tensile test

1. Introduction

The spheroidal graphite cast iron (FCD) for auto parts has been replacing the aluminum castings because of lightweighting the cars. However, the spheroidal graphite cast iron is now reviewed from the viewpoints of low price and recyclability. Therefore, making to high-valuable-addition is demanded for the spheroidal graphite cast iron more than before, and various studies such as thin wall castings have been done⁽¹⁾. By the way, the spheroidal graphite cast iron is difficult to weld because the carbon content of the iron base metal is high. Therefore, attempts to add nickel element and inoculation materials to the iron were made to enable welding⁽²⁾. In this case, however, the preheating of the iron base metal and the complicated processes of the postheating after welding are needed⁽³⁾⁽⁴⁾. Such a complicated welding has many problems on practical use. We have investigated to advance the surface decarburized spheroidal graphite cast iron (FCD-D). This material is a spheroidal graphite cast iron having thin decarburized surface layer, which is expected to be used in the car production line because neither the preheating nor the postheating processing of the base metal is needed and it can be easily welded. Up to now, the FCD-D has been produced by the solid decarburizing method, but

Table 1 Chemical composition of the FCD specimen used (mass%)

C	Si	Mn	P	S	Mg
3.70	2.73	0.16	0.015	0.005	0.042

there are such a lot of problems as long processing time etc.. To reduce the processing time the decarburization is studying to be done in the fluidized bed furnace. Some characteristics of decarburized layer are expected to be same in the cases of the solid decarburizing method and the fluidized bed furnace method. In this report, some characteristics of the surface decarburized spheroidal graphite cast iron produced by the solid decarburizing method are reported to clarify the practical usefulness in the car industry.

2. Experimental methods

The FCD materials used for the analysis of the decarburizing mechanism and the measurement of the mechanical properties were fabricated by casting. A chemical composition of the FCD material is shown in Table 1. The structure was a mixture of typical ferrite and pearlite structures having graphite particles dispersion.

2.1 Decarburizing of spheroidal graphite cast iron

In this study, the decarburizing was conducted by the heat-treatment for the solid decarburizing method. The iron oxide powder (FeO) and the test specimens (test pieces for tensile test and microstructure test) were filled into a steel pot (130 mm diameter and 130 mm in height), and it was heated at a speed of 13.1×10^{-3} K/s in a muffle furnace. After maintaining isothermally for 86.4–345.6 ks at elevated temperature of 973–1373 K, it was cooled at a speed of 89.7×10^{-3} K/s and was taken out from the furnace at 823 K. The specimens of the surface decarburized spheroidal graphite cast iron (FCD-D) were obtained by these treatments.

2.2 Shape of specimen

The specimens inserted in the steel pot are the test pieces for the tensile tests and the measurement of the thickness of decarburized layer. The tensile test specimens were shaped into a rod having a gauge part with 20 mm in length and 4, 6 and 8 mm in diameter. While the specimens to measure the thickness of decarburized layer were shaped into a block of 10 mm in width by 55 mm in length.

2.3 Measurement of thickness of decarburized layer

After heat-treatment for decarburizing, the test specimen was cut in half and the cut surface was polished to observe the microstructure by a scanning electron microscopy. The thickness of decarburized layer was determined from the decarburized layer region where the graphite particles had obviously disappeared.

2.4 Tensile test

The tensile test was conducted under an initial strain rate of 4.17×10^{-5} s⁻¹ at room temperature and the stress-strain curves were obtained. After the tensile test, the fracture surface of the specimen was observed by a scanning electron microscopy.

3. Results

3.1 Decarburized layer

Figure 1 shows the SEM photographs of the decarburized layer in the surface region of the specimens heat-treated for 288 ks at

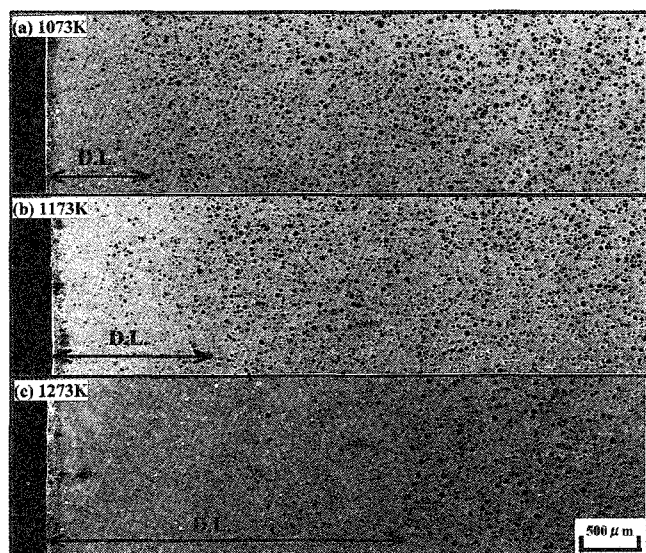


Figure 1 Scanning electron micrographs showing the formation of decarburized layer (D.L.) in the specimens heat-treated for 288 ks at (a) 1073 K, (b) 1173 K and (c) 1273 K.

1073, 1173 and 1273 K. The region of decarburized layer, D.L.. The decarburized layer means the region where the number of graphite decreases obviously. The thickness of the decarburized layer was observed to increase with increasing the heating time at the same temperature. By the way, many voids are observed everywhere in the decarburized layer. The dispersion of voids seems to be very similar to that of graphite particles in the undecarburized layer. Therefore, it seems that these voids correspond to a kind of Kirkendall voids. In the iron matrix, carbon atoms and iron atoms diffuse interstitially and substitutionally, respectively. The diffusion rate of carbon atoms is extremely higher than that of iron atoms. Therefore it is thought that the volume of the voids could not be compensated by the diffusion of iron atoms. This is the reason for the Kirkendall voids.

Figure 2 shows the relation between the thickness of decarburized layer, d , and the holding time, t , of decarburized specimens at various temperatures. A straight linear relation holds

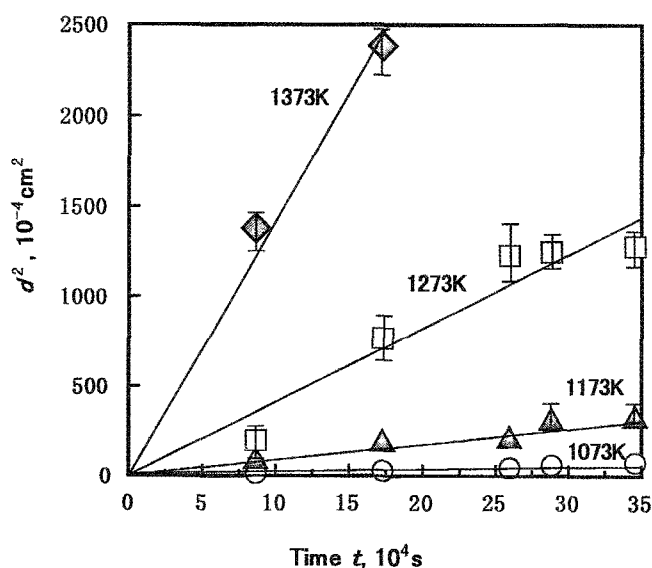


Figure 2 Relationship between the thickness of decarburized layer, d , and holding time, t , at various temperatures.

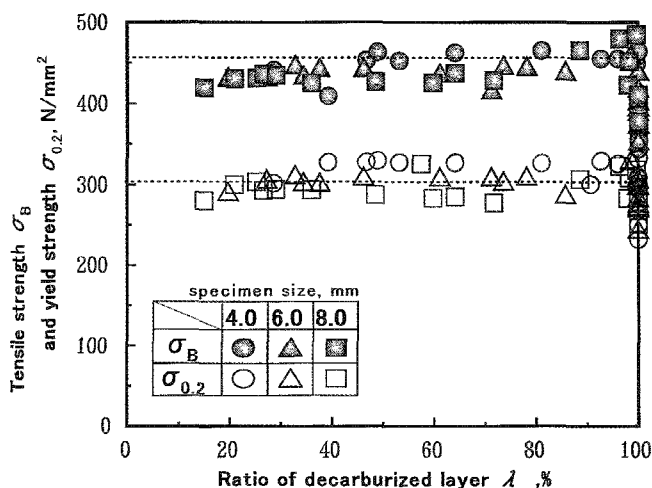


Figure 3 Relation among ratio of decarburized layer, tensile strength and yield strength of various specimens.

between d^2 and t on each temperature. Therefore, the rate controlling process for the growth of decarburized layer is presumed to be due to the carbon diffusion toward the surface side from inner side in the specimen. The details of the process will be discussed in chapter 4.

3.2 Tensile strength

Figure 3 shows relation among tensile strength, σ_B , yield strength, $\sigma_{0.2}$ and ratio of decarburized layer, λ of tensile specimens tested at room temperature. The values of σ_B and $\sigma_{0.2}$ do not depend on the ratio of decarburized layer and show almost constant values.

On the other hand, there is a very large scatter in the data at $\lambda=100\%$ in which the carburization of gauge part in the tensile specimen was conducted above 100%. This decarburized condition will be called as an overdecarburization. That is, the fully decarburized specimen was further continued to decarburize longer time for the overdecarburization.

Figure 4 shows the relation between the tensile strength and the excess time after full decarburization for various specimens. The tensile strength tends to decrease with increasing the heat-treatment time for overdecarburization.

4 Discussion

4.1 Growth of decarburized layer

From the results shown in Fig. 2, it was found that the following relation held between the thickness of decarburized layer, d , and the heating time for decarburization, t .

$$d^2=kt \quad (1)$$

Where, k is a rate constant. If the decarburization process to disappear the graphite particles is a single thermal activation process, k is represented by the following equation.

$$k=k_0\exp(-Q/RT) \quad (2)$$

Where, k_0 is a constant which does not depend on the temperature, R is a gas constant, Q is a activation energy for the graphite particles disappearance process and T is a heat-treatment temperature.

As for the disappearance process of the graphite particles, the following steps are thought: ① The carbon atoms dissolve into the

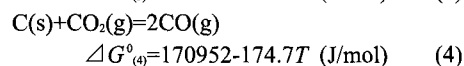
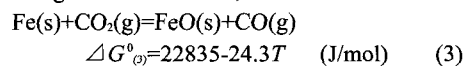
γ austenite phase from the graphite particle. ② The dissolved carbon atoms diffuse to the surface of specimen. ③ The carbon atoms are removed from the surface of specimen by a surface reaction. By the way, a linear relationship held between d^2 and t as shown in Fig. 2. Therefore, the step ② mentioned above is presumed to be a main part in the disappearance process of the graphite particles.

Figure 5 shows a liner relation between the logarithm of k and the reciprocal of the absolute temperature, T^{-1} , obtained from a result of Fig. 2. Therefore, the validity of equation (2) was evaluated by the experiment. From the result obtained the activation energy Q was calculated to be about 183.5 kJ/mol⁽⁶⁾. On the other hand, the activation energy for the diffusion of carbon atoms in the γ austenite phase is reported to be 157.0 kJ/mol. These values are almost similar. Therefore, the rate controlling process for the formation of decarburized layer is presumed to be due to the diffusion of carbon atoms toward the surface of the specimen, which dissolved into the γ austenite phase from graphite particles.

4.2 Mechanisms for graphite particles disappearance and oxide film formation

The decarburized layer was hardly obtained at 973 K in this study. Therefore, a critical temperature concerning the formation of decarburized layer is presumed to exist. This fact can be explained from the viewpoint of thermodynamics. Here, we will consider the oxidation reactions of the graphite and the γ austenite iron at the heating temperatures for decarburization.

According to the references,



Where, s shows the solid phase and g shows the gas phase. ΔG° shows the free energy change in the reactions, and T is an absolute temperature. In this experiment, the reaction of equation (3) is thought to occur in the steel pot. The free energy change of the reaction (3) in the steel pot is given by the following equation.

$$\Delta G_{(3)}=\Delta G^\circ_{(3)}+RT\ln(P_{\text{CO}}/P_{\text{CO}_2}) \quad (5)$$

Therefore, the value of $P_{\text{CO}}/P_{\text{CO}_2}$ in the atmosphere of steel pot can be calculated from equation (5). The calculated values are shown in Fig. 6.

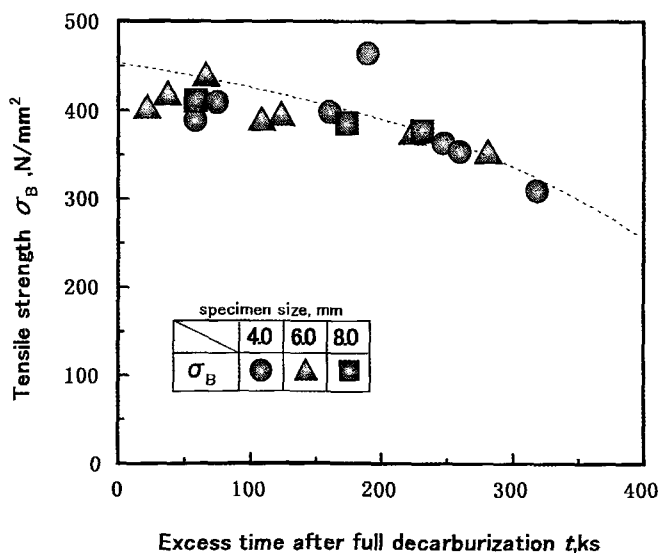


Figure 4 Relationship between excess time after full decarburization and tensile strength of various specimens.

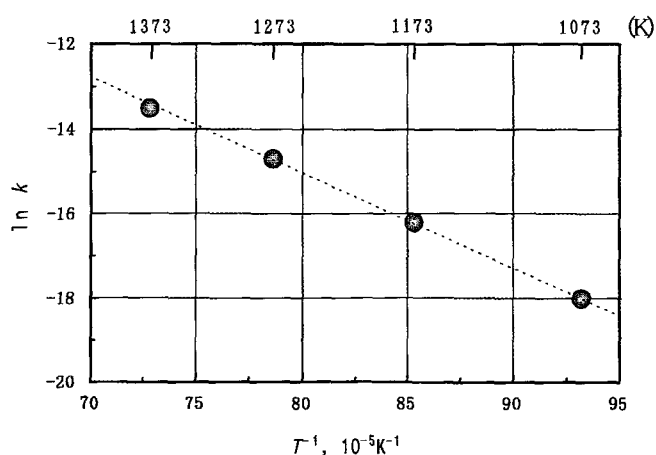


Figure 5 Relationship between the rate constant of decarburized layer, k , and temperature, T .

Figure 6 shows the relationship between $P_{\text{CO}}/P_{\text{CO}_2}$ in the steel pot atmosphere and temperature T , which was calculated from $\Delta G_{(3)}=0$ in the equation (5). It is understood that the value of $P_{\text{CO}}/P_{\text{CO}_2}$ tends to increase with increasing the temperature. This means that the test specimens were decarburized under this atmosphere in the steel pot.

The free energy change of the reaction (4) in the steel pot is given by the following equation.

$$\Delta G_{(4)} = \Delta G_{(4)}^0 + RT \ln(P_{\text{CO}}^2/P_{\text{CO}_2}) \quad (6)$$

Then, the value of $P_{\text{CO}}^2/P_{\text{CO}_2}$ under a unit pressure in the steel pot was obtained from the relation shown in Fig. 6. In addition, free energy changes of $\Delta G_{(3)}$ and $\Delta G_{(4)}$ for the reactions of (3) and (4) were calculated. The results obtained are shown in Fig. 7. In the steel pot, the reaction of equation (3) occurs under an equilibrium state. Therefore, the value of $\Delta G_{(3)}$ shows zero at any temperatures. On the other hand, it is known that the oxidation of carbon (equation (4)) is impossible below about 930 K because of $\Delta G_{(4)} \geq \Delta G_{(3)}=0$, though $\Delta G_{(4)}$ for equation (4) shows negative value at higher temperature side. This means the formation of FeO occurs dominantly below about 930 K. In the temperature range of this experiment the reaction of equation (4) is understood to occur dominantly because of $\Delta G_{(4)} \ll \Delta G_{(3)}=0$. Furthermore, the fact that the decarburized layer was not clearly confirmed at 973 K was well understood because the value of $\Delta G_{(4)}$ at 973 K was calcu-

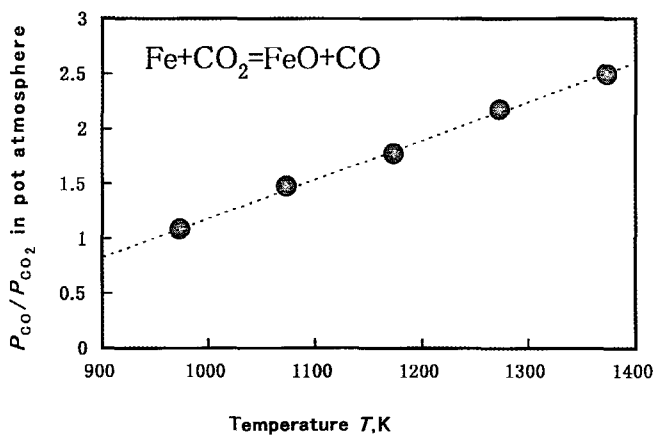


Figure 6 Relationship between the ratio of P_{CO} to P_{CO_2} in steel pot atmosphere and temperature, T .

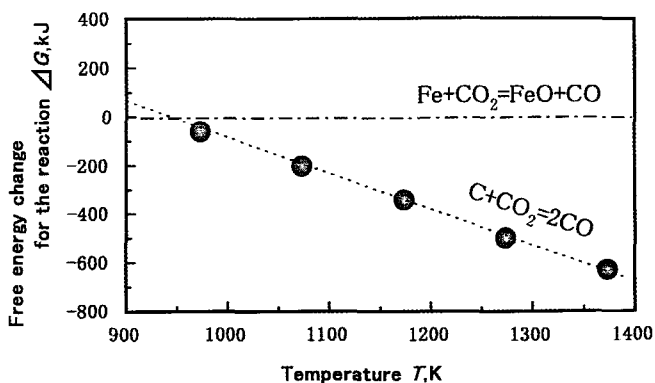


Figure 7 Relationship between free energy change for the reaction, ΔG and temperature, T .

lated to be -6.5 kJ/mol which was very close to zero.

In addition, we can understand from Fig. 7 that the formation of FeO film on the surface of γ austenite iron is expected below about 973 K.

4.3 Relation between tensile strength and decarburized layer

The sectional area in gauge portion of the rod shape tensile test specimen will be denoted by A . The area of decarburized layer region and undecarburized zone region in the section will be denoted by A_1 and A_2 , respectively. Then, the volume fraction of each region is given by $V_1=A_1/A$ for decarburized layer and $V_2=A_2/A$ for undecarburized zone. Therefore, the tensile stress of specimen is given by the following equation by using the rule of mixtures.

$$\sigma = \sigma_1 V_1 + \sigma_2 (1 - V_1) \quad (7)$$

Where, σ_1 and σ_2 show the tensile stress in the decarburized layer and in the undecarburized zone, respectively. Therefore, a linear relationship holds between σ and V_1 . In this experiment, the tensile strength did not depend on the ratio of decarburized layer and showed a constant value as shown in Fig. 3. Therefore, the following equation is given.

$$\sigma = \sigma_1 = \sigma_2 \quad (8)$$

Initially, we will consider the tensile strength σ_2 of the undecarburized layer. It is well known that the tensile stress of cast iron is lower than that of steel. This fact is due to the presence of graphite particles in the matrix of cast iron. There are a lot of studies on the effect of graphite particles on the tensile strength of cast iron, in which the values of tensile strength and elastic modulus of graphite are recognized to be 19.6 N/mm² and 4903 - 14710 N/mm², respectively. These values of graphite are remarkably low compared with those of iron matrix metal in the cast iron. Shiota⁽⁶⁾ explained the tensile strength of the spheroidal graphite cast iron as follows. Taking into account the notch effect and the strength of the particles, the tensile strength did not depend on the graphite particles but depend on the tensile strength of iron matrix part, σ_m , and the effective sectional area, A_{ef} . These ideas can be introduced in the result of this experiment. In the FCD material used in this experiment, the dispersion parameter of spheroidal graphite particles was determined to be 15.85 μ m in the average diameter and 37.34 μ m in the mean particle spacing. Therefore, because the effective sectional area of the matrix of iron was an area of the matrix of the iron of the unit area where one graphite existed, it was calculated to become 85.82% . σ_1 is given by the following equation as the Shiota's empirical formula.⁽⁶⁾

$$\sigma_1 = C \cdot \sigma_m \cdot A_{ef} \quad (9)$$

Where, C is a constant parameter due to notch effect and plastical restrain effect at around the graphite particle, σ_m is the tensile strength of iron matrix and A_{ef} is the effective sectional area.

From the literature⁽⁶⁾, $C \cdot \sigma_m = 543.3$ N/mm² and $\sigma_m = 523.7$ N/mm² are known in the case of ferrite matrix. Consequently, C is estimated to be 1.037 . Therefore, the notch effect and plastical restrain effect at around the graphite particle are presumed to be negligibly small. In the case of this experiment, the value of 466 N/mm² is calculated as the tensile strength, which is very close to the value obtained from Fig. 3.

This means that the tensile strength of undecarburized layer is determined from the value of A_{ef} in ferrite matrix and that the strength of dispersed graphite particles is negligibly small as voids.

Next discuss, the strength of decarburized layer. The graphite particles were decarburized to be voids and many voids were

confirmed in the decarburized layer. These voids have little strength. Therefore the effect of the dispersed voids on the tensile strength can be considered to be the same as that of dispersed graphite particles in the undecarburized layer. In a word, it is presumed that the tensile strength of decarburized layer, σ_1 , is identical to that of undecarburized layer, σ_2 . Therefore, it is reasonably understood that the tensile strength of the specimen does not depend on the ratio of decarburized layer but shows an almost constant value as shown in Fig. 3.

Consequently, it is concluded that the strength of graphite particles and voids do not directly depend on the strength of the FCD material but depend associating with the dispersion parameter of A_{ef} . Therefore, the fracture structure of undecarburized layer is expected to be similar to that of the decarburized layer. As an example, Figure 8 shows the microstructures of undecarburized region and decarburized region in the fracture surface of the tensile test specimen having the ratio of decarburized layer of 78%. As shown in Fig. 8, it is found that the dimple structure is formed in both of the regions and also that the size of dimples is almost same in both of the regions. These facts suggest that there is not any difference in the mechanical property of the both regions of specimen.

4.4 Decrease of strength due to overdecarburization

As shown in Fig. 4, it was found that the tensile strength decreased when the overdecarburization was processed. In the overdecarburizing process of the FCD-D material, following phenomena are thought to occur: ① Decreasing of the size and number of voids in the decarburized layer due to substitutional diffusion of iron atoms during the further heat-treatment after full decarburization, ② Decreasing of the carbon concentration in the decarburized layer due to the further decarburization.

If the phenomenon of ① occurs remarkably, the effective sectional area A_{ef} should be increased and the tensile strength should be increased as mentioned in equation (9). This fact is not consistent with the result of this experiment. On the other hand, the phenomenon of ② makes carbon-free state in the iron matrix.

By the way, it is well known that carbon atoms dissolve interstitially into the iron matrix lattice to occur solution hardening. For example, the tensile strength of the α Fe containing only 1.0×10^{-2} mass% of carbon is known to show 310 N/mm^2 ²⁷⁾. While, the tensile strength of the carbon free α Fe is known to show 265 N/mm^2 which is almost identical with the value of tensile strength extrapolated to the overdecarburizing time of 400 ks in Fig. 4. It is therefore concluded that the decrease in the tensile strength after overdecarburization is due to the phenomenon of ② mentioned above.

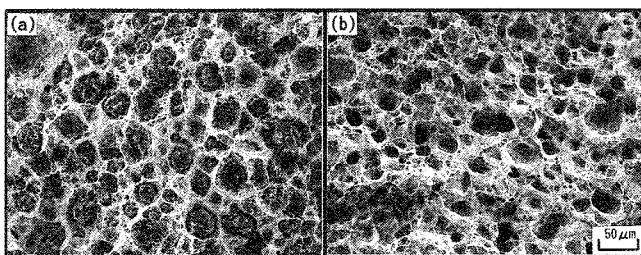


Figure 8 Scanning electron micrographs of (a) undecarburized region and (b) decarburized region in the fracture surface of tensile test specimen having the ratio of decarburized layer of 78%.

5. Conclusions

The rod-shaped spheroidal graphite cast irons (FCD) specimens having various diameters were decarburized for 86.4-345.6 ks at a temperature range from 973 to 1373 K. They were examined to clarify the decarburizing process and the mechanical properties of decarburized layer. The results obtained are as follows.

- (1) There is a critical temperature (930 K or less) for the decarburized layer formation. Below the temperature the decarburized layer is not formed.
- (2) During the decarburization, graphite particles disappear and change to voids which correspond to a kind of Kirkendall void caused by the difference in the diffusion coefficients for carbon and iron atoms in the γ austenite phase.
- (3) The activation energy for growth of the decarburized layer is estimated to be 183.5 kJ/mol which is very close to the value of the activation energy for diffusion of carbon atoms in the γ austenite iron.
- (4) The tensile strength of the decarburized FCD (FCD-D material) does not depend on the ratio of decarburized layers and shows a constant value of 455 N/mm^2 . This suggests that the graphite particles in the iron matrix can be regarded as the same as the voids in the decarburized layer.
- (5) After full decarburization, the tensile strength of the specimen decreases with increasing the heating time for overdecarburization. Therefore it is very important to note in the practical use of the FCD-D material so that the strength of thin parts decreases in the overdecarburized state.

References

- [1] The Japan Institute of Metals : Kinzoku Binran 946 Maruzen (2000).
- [2] Hiratsuka S., Horie H., Nakamura M., Kowata T., Aonuma M., Kobayashi T.: "TIG Welding of Spheroidal Graphite Cast Iron and Mild Steel Using the Inoculant Coated Welding Rods." J.Jap.Found. Eng. Soc. 70, 860-865 (1998).
- [3] Garlough G., Stoecker S.: "Ductile Iron Handbook" American Foundrymen's Society, INC252 (1993).
- [4] Pease G. R.: "The Welding of Ductile Iron" Suppl. Welding J. 1s-9s (1960).
- [5] Yamada S., Goto S., Aso S., Komatsu Y., Konno T.: "Growth Mechanism of Decarburized Layer in Spheroidal Graphite Cast Iron", J. Jap. Found. Eng. Soc. 73, 219-224, (2001).
- [6] Shiota T., Komatsu S.: "Relation between the Effective Sectional Area and the Static Strength of Cast Iron" IMONO49, 602-607, (1977).
- [7] Hiramatsu A., Yamada T.: "Predication of Stress-Strain curves in ferrite single structure steels", Iron Steel Inst. Jap. 263-268 (1994).